

Anthropomorphic Soft Pneumatic Fingers towards Full Dexterity of Human Hand*

Zihan Xu, Yu Bai, Runyu Ni, Ning Yang, Yi Sun, and Peng Qi, *Member, IEEE*

Abstract— Human fingers are highly dexterous due to the combination of multiple joints and degrees of freedom (DoFs). With the rise of soft material robots, many gripper prototypes have utilized soft robot technology. Nonetheless, it is still challenging to build a soft finger with a similar dexterity to human hand. Owing to the soft pneumatic actuator (SPA) fabrication flexibility, we have proposed a multiple DoFs soft pneumatic fingers design scheme that can mimic the motion patterns of human hand. Unlike the most SPA fingers where the motion patterns are fixed and limited, here our soft fingers can function like the human finger movements to a greater extent. The design is composed of three parts: (i) a SPA with two independent chambers as the main part of finger; (ii) a constraint layer made of unstretchable fabric which simulates tendon; (iii) a fiber-reinforced three-channel fluidic elastomer actuator (FEA). The abundance in DoFs expands the range of motions of the fingers and enables them to reach where human fingers can go. By controlling the internal pressure of the actuator, a variety of human finger motion patterns are achieved. Since each chamber's pressure can be individually controlled, the dexterous position control of the finger has been made possible. Fabrication process of the soft pneumatic fingers is presented, followed by the characterizations to provide a better understanding of their behaviors. In the last part of the article, a robotic hand composed of five fingers is fabricated for demonstration.

I. INTRODUCTION

Soft robotic gripper has drawn great attention from researchers over the past several years. In contrast to conventional rigid robotic grippers with solid actuators, soft robotic grippers are fabricated with soft materials and driven by soft media (e.g. pneumatic/hydraulic power and flexible cables). This new approach of bionic robot hand to provide safe human-robot-interaction for many challenging tasks. Among various daily activities, grasp task is undoubtedly one of the most common behaviors. Depending on the characters of object to be handled, various grasp types are proposed to ensure an adaptable grasp [1]. The traditional robotic grippers with rigid structural components have been proved to have difficulty working on these intuitive tasks. The minimum

application of compatible materials limits the capability of conventional robotic grippers, especially in applications where a safe and adaptable grasping is required (e.g. grasping of unknown objects or manipulation in undetected environments) [2]. The traditional rigid machine also has concern of limitation on gripping fragile and brittle object. In a recent study, the pneumatically actuated soft robot is tested, and a variety of soft grippers are developed [3], [4]. Evidences on development of pneumatically actuated soft robots have seen the expanded and improved performance of the grasping. In contrary to conventional robotic grippers, the pneumatically actuated grippers provide excellent versatility, ease of mass production and better safety and inherent compliance.

Many research groups have demonstrated successful applications of soft robot grippers. Ilievski *et al.* [3] provided one of the earliest bio-inspired soft-pneumatic grippers composed of six separate pneumatic actuators. Each pneumatic actuator inflates when compressed air is injected into the air chamber. A demonstration has also been made to exhibit the gesture of grasping an egg with six interactive actuators cooperating with each other. Aimed at dexterity grasping tasks, Deimel and Brock [4] proposed a novel pneumatic robotic hand. Their soft anthropomorphic hand uses silicone rubber and polyamide scaffolding to provide similar dexterity as human hand, and this innovative design is capable of accomplishing most of the human grasping tasks in the Feix taxonomy [5]. In a recent study, Manti *et al.* [6] developed a bioinspired cable-driven soft manipulator with the composition of three fingers, and it is more compliant to control than a pneumatic-driven gripper. Three soft fingers are made out of two types of silicone rubbers. Under the control of cables, this hand can grasp brittle objects with irregular shapes while preventing the damage to the surface of the objects. Another recent research of jamming principle presented by Brown *et al.* [7] evaluated a unique property of granular materials and its application as a basis for soft universal robotic gripper. A universal gripper is then developed to pick up objects with different sizes and shapes.

The current state-of-art soft robotic fingers are still incapable of mimicking the function of human fingers. Human finger is mainly composed of bones, joints and tendon, see Fig.1(a), while most of existing soft robotic fingers cannot simulate these biological components and thus can only be curved continuously and uniformly. The pneumatic robotic hand presented by Deimel and Brock [4] is composed of 7 actuators. Each actuator has one single chamber and hence limits the flexibility of motion. This type of single chamber design has a flaw of simulating the physiological structure of the human fingers. Taking the complexity of human finger movement into account, our design applies multiple independent chambers to imitate different joints in human

*Research sponsored by the Shanghai Sailing Program (17YF1420400) of Science and Technology Commission of Shanghai Municipality and the "Chenguang Program" (16CG20) of Shanghai Education Development Foundation and Shanghai Municipal Education Commission.

Z. Xu, Y. Bai, R. Ni, and P. Qi are with the Department of Control Science and Engineering, College of Electronics and Information Engineering, Tongji University, Shanghai, P. R. China. (corresponding author to provide e-mail: pqi@tongji.edu.cn).

N. Yang is with the George W. Woodruff School of Mechanical Engineering, Georgia Institute of Technology, 801 Ferst Drive, Atlanta, GA, 30332-0405, USA.

Y. Sun is with the Department of Mechanical Engineering and the Graduate School for Integrative Sciences and Engineering, National University of Singapore, Singapore 117575.

finger. Yang et al. [8] proposed a bioinspired robotic finger based on pneumatic actuator and shape memory polymer, however shape memory polymer can only provide single degree of freedom (DoF) while the metacarpo-phalangeal (MCP) joint of human finger has dual DoFs. To achieve dual DoFs, we use three fiber-reinforced fluidic elastomer actuators parallelly jointed together to mimic the MCP joint, so that the soft robotic finger can perform more complex and human-finger-like forms of motion. Furthermore, our design overcomes few disadvantages of shape memory polymer, such as long response time and high integration difficulty.

In this work, we propose a new soft pneumatic finger that possesses the same number and type of Dofs as human fingers. In our soft fingers, the DIP and PIP joints are realized by two independent pleated SPAs, and the MCP joint is achieved by a three-channel omni-directional FEA. Such configuration ensures similar movement and range of motions to human hand. We just reviewed relevant soft robotic finger and hand designs and discussed the differences among pre-works. Next, this article is organized as follows. The design and characterization of anthropomorphic soft hand is firstly presented. Three parts are differential by their physiological functions, namely, two-channel finger shell, constraint layer and three-channel-parallelly-jointed part. The fabrication method is also described with references. Secondly, we characterize the motion capabilities of the actuators in the finger individually and then demonstrate the grasping abilities of the five fingers after assembling into an anthropomorphic hand. Following the experiment section is conclusion and future work in Section IV.

II. DESIGN AND FABRICATION

A. Pneumatic Finger Design Principle

In order to build light and flexible soft robotic fingers capable of segmental bending and rotating, the hyper-elastic silicone rubber (Ecoflex 0030, Smooth-On) as the main material is chosen for the pneumatic fingers, and pressurized air as pneumatic power to achieve the bending and rotating capabilities. As illustrated by the conceptual design of the finger in Fig. 1, the current finger is 80 mm in length, 15 mm in width and 12 mm in height. (The two-channel pleated segment is 50 mm long and the length of three parallelly jointed fiber-reinforced fluidic elastomer actuators (FEAs) is 30 mm; the thumb is 60 mm in length because its pleated segment is 30 mm.) It can be seen in Fig. 1 that there are two chambers in the pleated segment, which are separated into two fluidic channels and can be controlled individually. These two joints mimic the proximal interphalangeal (PIP) joint and the distal interphalangeal (DIP) joint. Furthermore, to limit the heavy deformation of joints, each chamber is divided into two small cavities (13mm*1mm*11mm). When pressurized air is supplied, two small cavities will equally expand. The advantage of this special design is that the joint can avoid excessive deformation of a single cavity while reaching the desired bending angle. Other appurtenant, fingertip and bones are also simulated by silicone rubber in this segment.

In human fingers, tendon transforms actuation from muscle to actuate the finger. In our design, a constraint layer limits bending direction of soft robotic fingers. Therefore, it has a similar function as tendon. The metacarpo-phalangeal (MCP) joint of human fingers is not only capable of bending,

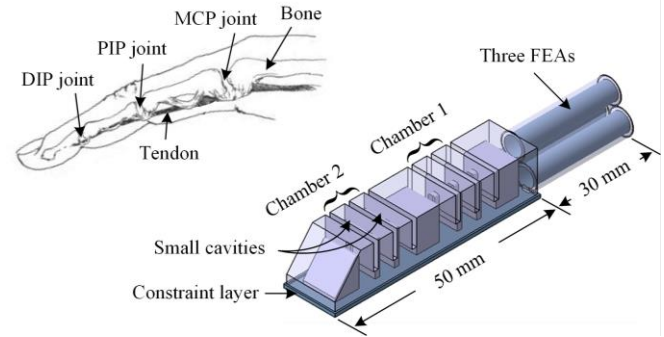


Figure 1. The design principle of an anthropomorphic soft pneumatic finger. Left: anatomic sketch of human index finger; Right: a conceptual representation of the designed finger.

but also can partially rotate the finger. To simulate this MCP joint, we design a continuum part which consists of three parallelly jointed fiber-reinforced fluidic elastomer actuators (FEAs) (see in Fig.1). These three fiber-reinforced channels are independent. By altering the inflated air chamber and the air pressure, the continuum part can achieve a 360° directional bending. Once the chambers are pressurized with modulated configuration of air pressure, the FEA can bend accordingly towards desired directions at targeted angles [9]. With cooperation of those three parts, different human finger's motion patterns can be performed with the designed soft robotic finger.

B. Pneumatic Finger Fabrication – Part I

The fabrication of a soft pneumatic actuator (SPA, using silicone rubber) is simple and economical, which makes it popular and wide used in the field [10]–[12]. In the first part of our scheme, we design two different sizes of 3D models, each having mold made up of two components (see Fig 2(a)). The molds are then assembled to be used in conjunction to make simulated fingers of difference lengths. The longer finger has two bending blocks with embedded air chambers (see Fig. 2(c-f)). The short finger has only one bending block with embedded air chamber to mimic the thumb, which has only one joint (see Fig. 2(g-h)). A layer of unstretchable fabric coated with silicone-rubber is glued to the bottom surface. This layer only allows tiny plane strain which can be neglected. As a result, the pressurization of the air chamber expands at the embedded chamber, while the strain on the bottom surface remains zero. This produces a bending motion in which the distance between the two connections of the curved block decreases as the curvature increases [10].

Detailed fabrication process is given as follows. Firstly, Ecoflex A and B part are mixed in equal volume by centrifugal mixer (SIENOX® SIE-C500-2F). After vacuuming the mixture, the mixture is cast into the PLA plastic molds in (see Fig. (b)). These molds are prepared using 3D printer (LULZBOT®, Taz 6). Silicon rubber is solidified either at the room temperature for about 2 hours or at 50 degrees Celsius for about 30 minutes. Set the other part of the mold to the one that already filled with silicone, and then the rib plate is used to get the shape of the finger and the air chamber. The constraint layer is fabricated by applying the degassed silicone rubber evenly on a piece of fabric [10]. In human fingers, motion of bending relies on the tendons of the inner surface of

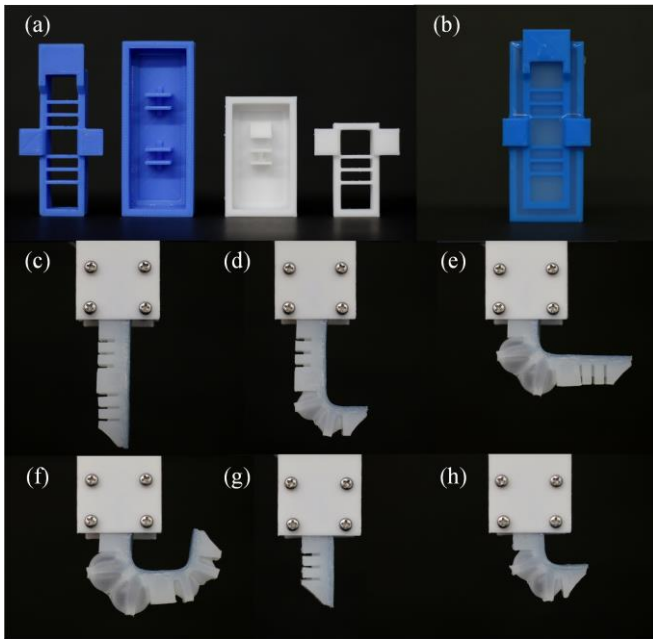


Figure 2. Fabrication of the pleated segment as pneumatic fingers. (a) Molds two sizes of 3D models; (b) the mixture casted into PLA plastic molds; (c)-(f) actuations of the longer two-chamber finger; (g)-(h) actuations of the shorter single chamber finger.

the finger. The role of the constraint layer is to mimic the tendons of human fingers. while inflating the air chamber embedded in the finger, the silicone-based elastomer actuator deforms uniformly in the trend of air pressure [6], whereas the constraint layer has no deformation. The difference in the deformation achieve the bending motion analogous to human finger bending. When cured, the constraint layer is trimmed, and two thin silicone tubes (with external diameter of 1 mm) are placed in the pre-retained channel and connected to two individual chamber sets so that these two joints can be controlled separately.

C. Pneumatic Finger Fabrication – Part II

The continuum part that bends in three dimensions upon pressurization and imitates metacarpo-phalangeal (MCP) joint of human finger is fabricated by composing flexible elastomers with different tensile strengths using soft lithographic molding. Each joint is made up of three chambers bonded with silicone rubber adhesive.

This fabrication process in detail is illustrated in Fig. 3. The mixed and degassed silicone prepolymer was casted into a new cylindrical mold (Fig. 3(a)). Before the silicon rubber is solidified, insert a fine carbon rod ($\Phi = 3.5\text{mm}$) into the mold. A central hole in the lid and a circular groove at the bottom of the tube ensure concentric position of the rod. After solidification, the fine carbon rod is carefully pulled out of the rubber (see Fig. 3(b)).

Then, it is the thread winding process (see Fig. 3(d)). In previous work, the threads or fibers are wound manually [4], [13], [14]. Manual work can hardly achieve the consistent low-pitch winding, whilst it is required in our case, as the fiber reinforced actuator will be casted again and pulled out from the PLA plastic mold. If the filament winding is uneven, the gap will increase significantly in the next process of pulling

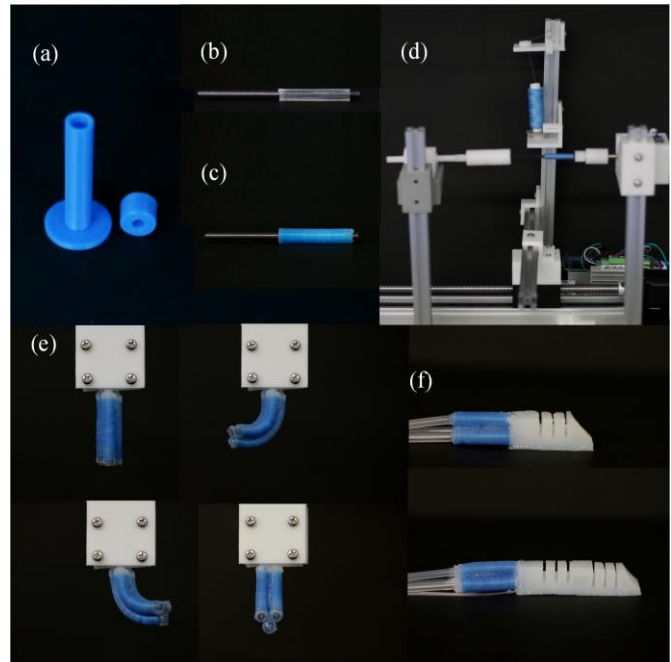


Figure 3. Fabrication of a short continuum fiber-reinforced fluidic elastomer actuator (FEA). (a) mold for making the inner silicone layer; (b) ready-made inner silicone layer; (c) ready-made FEA; (d) fiber reinforcement by winding machine. (e) three parallelly jointed FEAs; (f) fabricated fingers.

out the fiber-reinforced tube from the second PLA plastic mold, thus a large deformation in the gap when it inflates will prevent the actuator from achieving a uniform bending.

We customized a winding machine (see Fig. 3(d)) composing two motors. Driven by two motors, the thread feeder is moving slowly relative to the rotating object. By programming the steps and clock cycle of the two motors respectively, we can select the appropriate winding length, winding pitch and fiber layers to eventually form a suitable reinforcement. Therefore, for thread winding, we used an automated winding machine and applied two layers of cotton thread winding (thickness = 0.15 mm, max strain < 1%) and a 4-mm pitch set of linear guide to uniformly wind the entire silicone body which avoids the local inflation effectively. During the winding process, the thread tension was minimized by the low friction between the slider and linear guide and the slow rotation velocity of actuator. The remaining tension in our winding process is small enough to prevent deformation of silicone body. Yet the actuator diameter is slightly slimmed down by about 0.3 mm.

After the winding process, we spread a thin layer of silicone on fiber layers to secure the position of the threads. Then the actuator is placed into a vacuum chamber to degas the cotton threads. After the wired actuator is cured, it is again casted into a PLA plastic mold, which has the same shape as the mold in Fig. 3(a) but with a larger diameter. with another mixing-injecting-curing process, the fiber-reinforced fluidic elastomer actuator with one chamber is fabricated (see Fig. 3(c)). Three same actuators are bonded together with silicone rubber adhesive (SMOOTH-ON, Inc. Sil-Poxy) to form a continuum part, which mimics the MCP joint of human finger (see Fig. 3(e)). Although the continuum part seems like a short finger, in our design scheme this continuum part only

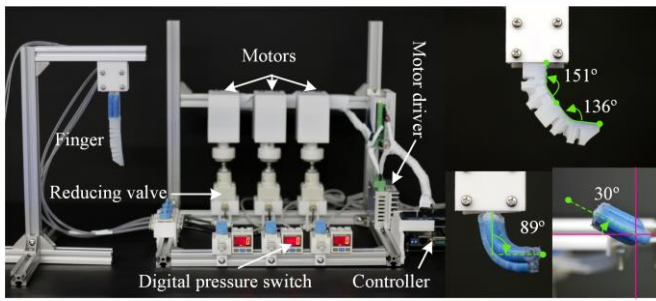


Figure 4. Experimental setup. It composes three motors and three pressure regulators; the pressures of the three-channel airway are measured by digital pressure switches.

functions as the MCP joint. Lastly, three silicone tube (with external diameter of 4 mm) is inserted into three chambers respectively and the other side of fluidic elastomer actuator is glued to the pleated segment, the whole fabrication is completed After the connection to the fore-part of finger (see Fig. 3(f)).

III. EXPERIMENT

To understand the characteristics of this soft pneumatic finger, experiments with a series of measurements are conducted to figure out the relationships between the bending direction/angle and the different pressure values (see Fig. 4 and Fig. 5). After analyzing the local behavior of a finger, the evaluation of the dexterous grasping capabilities of the proposed hand is conducted (see Fig. 6). For the real-world grasping experiments, we focus on evaluating the grasp capabilities offered by this multi-DoFs pneumatic fingers. As the deformation of the loaded finger is unpredictable, it is difficult to simulate the grasping accurately. For this consideration, we introduced empirical methods to define the evaluations and validate the values.

A. Measurement Setup

In general, the physical model of the elastic pneumatic actuator based on silicone can be described by the function of air pressure and bending angle. The curvature of the soft finger when the air chamber is subjected to pressure is measured for quantitative analysis. To characterize the performance of the soft robotic fingers, we customized an experimental setup composing three motors and three pressure regulators (see Fig. 4). The pressures of the three-channel airway are measured by digital pressure switches (SMC[®], ZSE30A(F)). The main controller of the control machine is the development board (ALIENTEK[®], APOLLO) using the stm32f429 MPU (Microprocessor Unit). Since the pin voltage of the stm32f429 MPU is 3.3V and the direction control signal of the motor requires at least 5V voltage, conventional approach can be used to solve this dilemma, such as using drive chips L298N. This is the ST production high integrated of a Dual-H bridge motor driver chip, hence the connection circuit is simple. Its output voltage is adjustable by PWM input signal to meet the requirements. Here, we use Arduino Mega development board to get the driver signal, the output voltage of Arduino MEGA is 5 V and can work well.

B. Characteristics of Bending Angles and Directions

As a pivotal feature of soft pneumatic finger, the bending capability is studied, and the measurement results are represented below. To have a better understanding of the response of the soft pneumatic fingers to different input pressures, we apply different air pressures and record its corresponding bending directions. The whole measurement setup is shown in Fig. 4, and the ready-made finger is fixed on the adjustable fixture.

Taking the Mullins effect of elastomer [15] into consideration, the soft pneumatic fingers are pre-actuated five

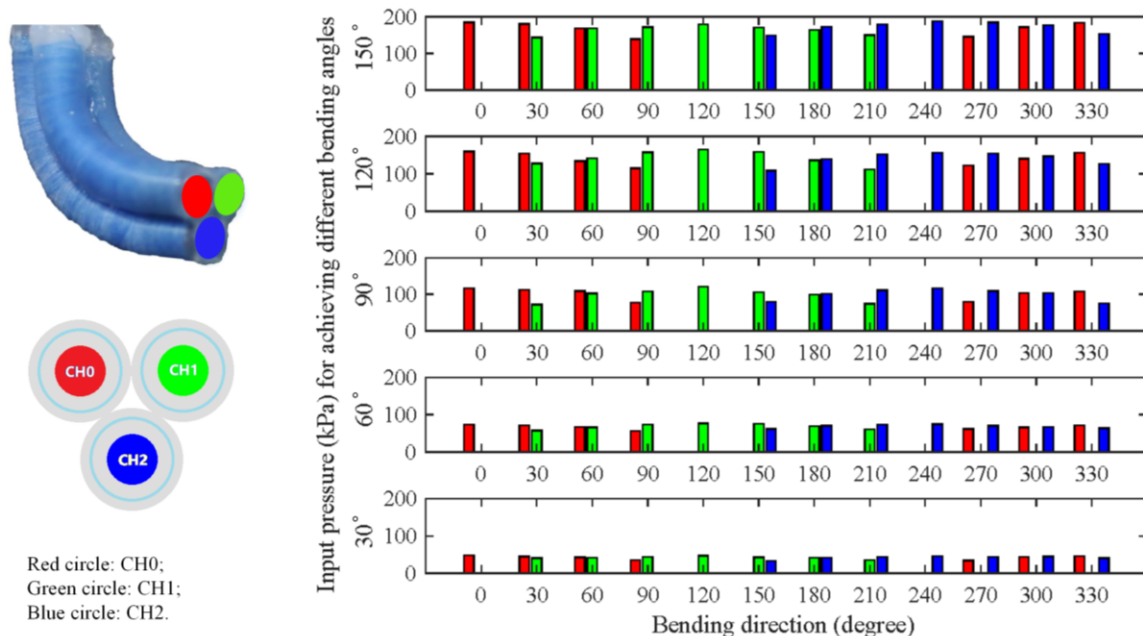


Figure 5. Measurement results for actuating the fiber-reinforced FEAs under different bending angles and directions.

TABLE I. BENDING ANGLE MEASUREMENT RESULTS

Forefinger DIP joint						
		10°	30°	50°	70°	90°
1st	Unit (kPa)	3.828	11.484	11.851	13.143	13.821
2nd		3.290	10.662	11.834	12.283	13.343
3rd		3.689	10.690	13.062	13.865	14.237
Mean		3.602	10.945	12.249	13.097	13.800
SD		0.279	0.467	0.704	0.792	0.447
Forefinger PIP joint						
		10°	30°	50°	70°	90°
1st	Unit (kPa)	3.334	10.631	12.867	13.365	14.120
2nd		3.114	9.737	12.853	13.346	14.809
3rd		2.258	10.249	12.139	12.711	14.904
Mean		2.902	10.206	12.620	13.141	14.611
SD		0.568	0.449	0.416	0.372	0.428
Middle finger DIP joint						
		10°	30°	50°	70°	90°
1st	Unit (kPa)	1.211	4.461	7.320	10.446	10.730
2nd		1.270	4.384	8.651	10.097	10.817
3rd		1.154	4.396	7.630	10.468	11.187
Mean		1.212	4.414	7.867	10.337	10.911
SD		0.058	0.041	0.696	0.208	0.243
Middle finger PIP joint						
		10°	30°	50°	70°	90°
1st	Unit (kPa)	2.641	9.613	11.298	11.834	12.214
2nd		2.461	9.608	11.142	11.763	12.385
3rd		2.762	9.862	11.220	11.848	12.494
Mean		2.621	9.694	11.220	11.815	12.364
SD		0.151	0.145	0.078	0.046	0.141
Ring finger DIP joint						
		10°	30°	50°	70°	90°
1st	Unit (kPa)	2.267	4.746	8.597	9.756	10.446
2nd		1.892	4.935	8.601	10.552	10.566
3rd		1.918	4.618	8.574	9.667	10.483
Mean		2.026	4.766	8.591	9.992	10.498
SD		0.209	0.159	0.015	0.487	0.061
Ring finger PIP joint						
		10°	30°	50°	70°	90°
1st	Unit (kPa)	2.692	9.426	11.738	12.297	13.711
2nd		2.569	9.472	11.489	12.478	13.689
3rd		2.656	9.511	11.850	12.514	13.956
Mean		2.639	9.470	11.692	12.430	13.785
SD		0.063	0.043	0.185	0.116	0.148
Little finger DIP joint						
		10°	30°	50°	70°	90°
1st	Unit (kPa)	2.105	6.198	9.241	13.474	14.180
2nd		2.278	6.325	9.309	13.205	14.426
3rd		2.582	6.292	9.115	15.501	14.079
Mean		2.322	6.272	9.222	14.060	14.228
SD		0.241	0.066	0.098	1.255	0.178
Little finger PIP joint						
		10°	30°	50°	70°	90°
1st	Unit (kPa)	3.238	9.805	14.347	16.650	17.324
2nd		3.558	9.903	14.384	16.564	17.444
3rd		3.410	9.879	14.372	16.745	17.289
Mean		3.402	9.862	14.368	16.653	17.352
SD		0.160	0.051	0.019	0.091	0.081

Thumb joint						
		10°	30°	50°	70°	90°
1st	Unit (kPa)	2.909	6.816	11.569	14.467	15.417
2nd		2.426	7.052	11.592	14.389	15.270
3rd		2.712	6.854	11.623	14.313	15.386
Mean		2.682	6.907	11.595	14.390	15.358
SD		0.243	0.127	0.027	0.077	0.077

times before measuring. This allows the silicone material to approach the constant stress-strain characteristics. Immediately after the pre-actuation, the bending tests for each finger are repeated. In terms of the bending angle for the two-channel pleated segment, we set the bending angle range from 10° to 90° with 20° of increments, and then record the corresponding air pressure for each bending configuration. For fiber-reinforced fluidic elastomer actuators, we set the bending direction from 0° to 330° with 30° of increments and the bending angles from 30° to 150° with 30° of increments. For accuracy purpose, five samples are measured three times each. The bending angles are measured in pictures using motion analysis software: tracker [16] (see Fig. 4) and all the values are recorded in Tab. I (for the two-channel pleated segment) and in Fig. 5 (for the fiber-reinforced FEAs).

In Tab. I, it shows the measured mean pressure and the standard deviation for 9 joints at different bending angles. Overall, as the bending angle increases, the air pressure for all joints increases. However, there are also some unexpected results. It is seen from Tab. I that the pressure values required by the same joint of the different fingers to reach the same bending angle vary greatly. For example, the air pressure needed by little finger PIP joint to reach 90° is above 17 kPa, while for other joints, this pressure value is not more than 15 kPa. The reason for this feature is that the production process of little finger from other fingers differs. Furthermore, the standard deviation is randomly distributed across the joints. In other words, the bending repeatability of the joint needs to be improved. The possible reason for this feature is the uncontrollable chamber inflation and their interactions between two pressurized chambers (see Fig. 2(e)).

The measurement results for actuating the fiber-reinforced FEAs are presented in Fig. 5. We use red bar, green bar and blue bar to represent air channel 1, 2 and 3 of these three FEAs. It can be seen that in each bending direction a large bending angle always requires a higher pressure even sometimes with multiple channels. In each row, the bending directions on 0°, 120° and 240° need a single channel actuated. The direction of single-single-channel-actuated bending can be changed in the reverse direction when other two air channels are actuated identically with the same pressure. The three-chamber actuation manner can achieve a rotation as a ball joint. From a bionic point of view, it can mimic the movement of human MCP joint on a two-dimensional plane by applying model-free adaptive control strategy.

C. Analysis of Motion Similarities

Imitation ability is based on the bending shape control. Since we have five chambers in each finger whilst three chambers in each fiber-reinforced FEA cannot expand at the

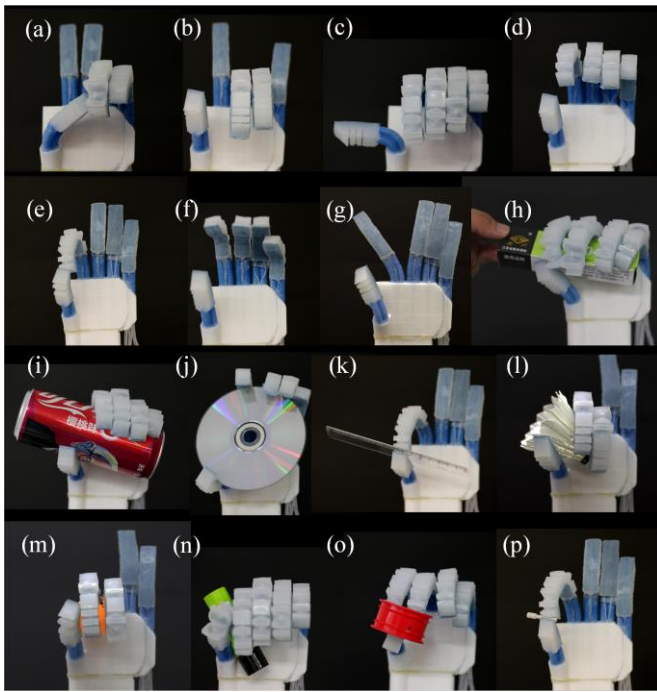


Figure 6. The demonstrations of the anthropomorphic hand featuring our soft pneumatic fingers. (a)-(g): the daily hand gestures made by the anthropomorphic hand, (h)-(p): various grasping modes realized by the anthropomorphic hand in grabbing objects of distinctive shapes and sizes.

same time. Hereby, we eventually have 27 different combinations for motion patterns in each finger (k -combinations: $C_5^4 - 2 + C_5^3 - 1 + C_5^2 + C_5^1 = 27$). Thumb has less motion patterns ($C_4^3 - 1 + C_4^2 + C_4^1 = 13$) since its pleated segment has only one chamber. Considering the fact that one hand has five fingers, there are still lots of motion patterns to be achieved. In this article, we chose several common gestures to testify the imitation ability of our soft pneumatic finger, as seen in Fig. 6. In this preliminary demo, all fingers are anchored into a 3D-printed anthropomorphic rigid palm. Here, the dexterous grasping capabilities of this “hand” can also be illustrated via grasping different shapes of objects, while the conventional rigid hands and other single-channel soft hands can hardly achieve them all.

IV. CONCLUSION AND FUTURE WORK

Dexterity or the controllability of position is the primary requirement in soft robotic hand for reliable and predictable operations in practical applications. Most soft pneumatic fingers have no bionic structure so their motion patterns are limited. This work proposes a novel anthropomorphic soft pneumatic finger along with its fabrication method. By controlling air pressure of discrete joints, the bending angle and direction of joints are controlled separately for dexterous grasps. The proposed fabrication method can be expended to build more flexible bionic rotary joints which exhibit potential for precise bending position control in various applications since rotation angles can be controlled precisely. Meanwhile, experiments are conducted to examine independent joint position control and rotation control

abilities of the finger and the dexterity of our soft pneumatic fingers is verified.

For future study, design and fabrication will be improved in order to make the chamber inflation more regular and the bending performance more repeatable. In the meantime, a reliable model of the hand will be established to design its behaviors for different gestures. So far, our work has only been modeled on bones, joints and tendons of finger, palm and neural networks including skin are still not imitated. In future work, appropriate pressure sensors will be attached to the finger to provide contact surface pressure feedback like human skin so that more complicated grasping tasks could be performed. Furthermore, soft pneumatic palm will also be designed to cooperate with the fingers to complete the dexterous grasping task.

REFERENCES

- [1] A. M. Dollar, “Classifying human hand use and the activities of daily living,” *The Human Hand as an Inspiration for Robot Hand Development*, R. Balasubramanian and V. J. Santos, Ed., New York: Springer, pp. 201–216, 2014
- [2] D. Rus and M. T. Tolley, “Design, fabrication and control of soft robots,” *Nature*, vol. 521, pp. 467–475, 2015.
- [3] F. Ilievski, A. D. Mazzeo, R. F. Shepherd, X. Chen, and G. M. Whitesides, “Soft robotics for chemists,” *Angewandte Chemie*, vol. 50, no. 8, pp. 1890–1895, 2011.
- [4] R. Deimel and O. Brock, “A novel type of compliant and underactuated robotic hand for dexterous grasping,” in *Proc. Robotics: Science and Systems*, Berkeley, USA, 2014, pp. 1687–1692.
- [5] T. Feix, J. Romeo, H. Schmiebmayer, A. M. Dollar, and D. Kragic, “The GRASP taxonomy of human grasp types,” *IEEE Trans. Hum-Mach. Syst.*, vol. 46, no. 1, pp. 66–77, 2016.
- [6] M. Manti, T. Hassan, G. Passetti, N. D’Elia, C. Laschi, and M. Cianchetti, “A bioinspired soft robotic gripper for adaptable and effective grasping,” *Soft Robotics*, vol. 2, no. 3, pp. 107–116, 2015.
- [7] E. Brown, N. Rodenberg, J. Amend, A. Mozeika, E. Steltz, M. R. Zakin, H. Lipson, and H. M. Jaeger, “Universal robotic gripper based on the jamming of granular material,” *PNAS*, vol. 107, no. 44, pp. 18809–18814, 2010.
- [8] Y. Yang, Y. Chen, Y. Li, Michael Z. Q. Chen, and Y. Wei, “Bioinspired robotic fingers based on pneumatic actuator and 3D printing of smart material,” *Soft Robotics*, vol. 4, no. 2, pp. 147–162, 2017.
- [9] Y. Sun, S. Song, X. Liang, and H. Ren, “A miniature soft robotic manipulator based on novel fabrication methods,” *IEEE Robot. Autom. Letters*, vol. 1, no. 2, pp. 619–623, 2016.
- [10] Y. Sun, Y. S. Song, and J. Paik, “Characterization of silicone rubber based soft pneumatic actuators,” in *Proc. IEEE Int. Conf. Intell. Robots Syst*, Tokyo, Japan, 2013, pp. 4446–4453.
- [11] Y. Sun, K. Wu, C. M. Lim, and H. Ren, “Soft oral interventional rehabilitation robot based on low-profile soft pneumatic actuator,” in *Proc. IEEE/RSJ Int. Conf. Rob. Autom.*, Seattle, USA, 2015, pp. 2907–2912.
- [12] Y. S. Song, Y. Sun, R. van den Brand, J. von Zitzewitz, S. Micera, G. Courtine, and J. Paik, “Soft robot for gait rehabilitation of spinalized rodents,” in *Proc. IEEE Int. Conf. Intell. Robots Syst.*, Tokyo, Japan, pp. 971–976, 2013.
- [13] P. Polygerinos, Z. Wang, J. Overvelde, K. C. Galloway, R. J. Wood, K. Bertoldi and C. J. Walsh, “Modeling of soft fiber-reinforced bending actuators,” *IEEE Trans. Robot.*, vol. 31, no. 3, pp. 778–789, 2015.
- [14] F. Connolly, P. Polygerinos, C. J. Walsh, and K. Bertoldi, “Mechanical programming of soft actuators by varying fiber angle,” *Soft Robotics*, vol. 2, no. 1, pp. 26–32, 2015.
- [15] S. Cantournet, R. Desmorat, and J. Besson, “Mullins effect and cyclic stress softening of filled elastomers by internal sliding and friction thermodynamics model,” *Int. J. Solids and Structures*, vol. no. 11–12, 46, pp. 2255–2264, 2009.
- [16] [Online]. Available: <http://physlets.org/tracker/>